

Communication

Spatially varying steady state longitudinal magnetization in distant dipolar field-based sequences

C.A. Corum*, A.F. Gmitro

Optical Sciences Center, University of Arizona, AHSC, P.O. Box 245067, Tucson, AZ 85724-5067, USA

Received 1 April 2004; revised 28 July 2004

Available online 17 September 2004

Abstract

Sequences based on the distant dipolar field (DDF) have shown great promise for novel spectroscopy and imaging. Unless spatial variation in the longitudinal magnetization, $M_z(s)$, is eliminated by relaxation, diffusion, or spoiling techniques by the end of a single repetition, unexpected results can be obtained due to spatial harmonics in the steady state $M_z^{ss}(s)$ profile. This is true even in a homogeneous single-component sample. We have developed an analytical expression for the $M_z^{ss}(s)$ profile that occurs in DDF sequences when smearing by diffusion is negligible in the TR period. The expression has been verified by directly imaging the $M_z^{ss}(s)$ profile after establishing the steady state.

© 2004 Elsevier Inc. All rights reserved.

PACS: 82.56.Jn; 82.56.Na; 87.61.Cd

Keywords: Distant dipolar field; DDF; Intermolecular multiple quantum coherence; iMQC; Steady state longitudinal magnetization

1. Introduction

NMR and MRI sequences utilizing the distant dipolar field (DDF) have the relatively unique property of preparing, utilizing, and leaving spatially modulated longitudinal magnetization, $M_z(s)$, where \hat{s} is in the direction of an applied gradient. In fact this is fundamental to producing the novel “multiple spin echo” [1,2] or “non-linear stimulated echo” [3] of the classical picture and making the “intermolecular multiple quantum coherence (iMQC)” [4] observable in the quantum picture.

Existing analytical signal equations for DDF/iMQC sequences depend on $M_z(s)$ being sinusoidal during the signal build period [5,6]. Experiments that probe sample structure also require a well-defined “correlation distance” which is defined as the repetition distance of

$M_z(s)$ [7–9]. If the repetition time TR of the DDF sequence is such that full relaxation is not allowed to proceed $TR < 5T_1$, or diffusion does not average out the modulation, spatially modulated longitudinal magnetization will be left at the end of one iteration of the sequence. The next repetition of the sequence will begin to establish “harmonics” in what is desired to be a purely sinusoidal modulation pattern. Eventually a steady state is established, potentially departing significantly from a pure sinusoid.

2. Experimental methods

To study the behavior of the steady state $M_z^{ss}(s)$ profile, we have implemented a looped DDF preparation subsequence followed by a standard multiple-phase encode imaging sub-sequence. (Fig. 1.) The α pulse excites the system, the gradient G_q twists the transverse magnetization into a helix. β rotates one component of the helix back into the longitudinal direction. For simplicity

* Corresponding author. Fax: +520 626 3893.

 E-mail address: corum@email.arizona.edu (C.A. Corum).

 URL: <http://www.u.arizona.edu/~%7Ecorum>.

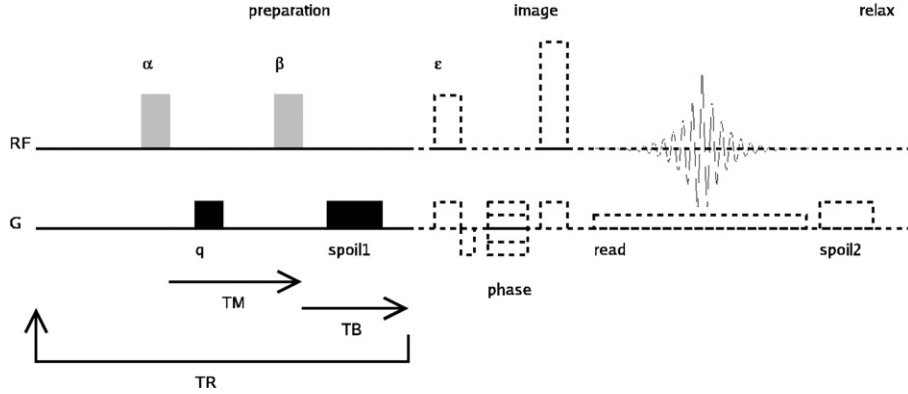


Fig. 1. Pulse Sequence. All RF pulses shown as hard for simplicity are actually Sinc3. α and β are the same phase.

we have omitted the 180° pulses used to create a spin echo during TM and/or TB sometimes present in DDF sequences. The “preparation” sub-sequence creates the periodic $M_z(s)$ profile, spoils remaining transverse magnetization, and after repeated looping establishes the steady state $M_z^{SS}(s)$. The ϵ pulse converts $M_z^{SS}(s)$ into transverse magnetization, allowing it to be imaged via the subsequent spin echo “image” sub-sequence. $M_z^{SS}(s)$ must be re-established by the “preparation” sub-sequence for each phase encode. After a suitably long full relaxation delay “relax,” the sequence is repeated to acquire the next k -space line.

Note that we are only interested in $M_z^{SS}(s)$ in this experiment, not the actual DDF-generated transverse signal (which we spoil with the “spoil1” gradient). This is clearly a slow acquisition method because many TR periods are required to reach steady state in the preparation before each k -space line is acquired. Re-establishing the steady state is required for each phase encode because the ϵ pulse converts the $M_z^{SS}(s)$ profile into transverse magnetization so that it can be imaged. The sequence is intended as a tool to directly image the $M_z^{SS}(s)$ profile, verifying the $M_z^{SS}(s)$ that would occur in a steady state DDF sequence, not as a DDF imaging method.

3. Theory

The effect of the “preparation” pulse sequence was first determined for a single iteration. The progress along the sequence is denoted by the superscript.

Starting with fully relaxed equilibrium magnetization before the α pulse

$$M_z^{\text{Eq}}(s) = M_0 \quad (1)$$

after the α pulse, the mix delay TM and the β pulse we have:

$$M_z^\beta(s) = [A^\beta \cos(qs) + B^\beta] M_z^{\text{Eq}} + C^\beta M_0, \quad (2)$$

$$A^\beta = -\sin(\alpha) e^{-\frac{TM}{T_2}} \sin(\beta),$$

$$B^\beta = \cos(\alpha) e^{-\frac{TM}{T_1}} \cos(\beta),$$

$$C^\beta = (1 - e^{-\frac{TM}{T_1}}) \cos(\beta).$$

The parameter $q = 2\pi/\lambda$, where λ is the helix pitch resulting from the applied gradient. Diffusion has been assumed to be negligible at the scale of λ . Note that T_2 is used in A rather than T_2^* when G_q is significantly larger than background inhomogeneity and susceptibility gradients.

After the build delay TB we have:

$$M_z^{\text{TB}}(s) = [A^{\text{TB}} \cos(qs) + B^{\text{TB}}] M_z^{\text{Eq}}(s) + C^{\text{TB}} M_0, \quad (3)$$

$$A^{\text{TB}} = -\sin(\alpha) e^{-\frac{TM}{T_2}} \sin(\beta) e^{-\frac{TB}{T_1}},$$

$$B^{\text{TB}} = \cos(\alpha) e^{-\frac{TM}{T_1}} \cos(\beta) e^{-\frac{TB}{T_1}},$$

$$C^{\text{TB}} = [(1 - e^{-\frac{TM}{T_1}}) \cos(\beta) - 1] e^{-\frac{TB}{T_1}} + 1.$$

At the start of the next repetition, after a TR period inclusive of TM and TB we have:

$$M_z^{\text{TR}}(s) = [A^{\text{TR}} \cos(qs) + B^{\text{TR}}] M_z^{\text{Eq}}(s) + C^{\text{TR}} M_0, \quad (4)$$

$$A^{\text{TR}} = -\sin(\alpha) e^{-\frac{TM}{T_2}} \sin(\beta) e^{-\frac{TR-TM}{T_1}},$$

$$B^{\text{TR}} = \cos(\alpha) \cos(\beta) e^{-\frac{TR}{T_1}},$$

$$C^{\text{TR}} = [(1 - e^{-\frac{TM}{T_1}}) \cos(\beta) - 1] e^{-\frac{TR-TM}{T_1}} + 1.$$

If we apply the sequence N times and re-arrange the terms we get the series:

$$M_z^{N \times \text{TR}}(s) = M_0 + M_0 [A^{\text{TR}} \cos(qs) + B^{\text{TR}} + C^{\text{TR}} - 1] \times \sum_{n=1}^N [A^{\text{TR}} \cos(qs) + B^{\text{TR}}]^{n-1} \quad (5)$$

for the starting magnetization state after N repetitions of the sequence.

Summing an infinite number of terms results in the expression for the steady state $M_z^{SS}(s)$ after a large number of TR periods:

$$M_z^{SS}(s) = M_0 - M_0 \left[\frac{A^{TR} \cos(qs) + B^{TR} + C^{TR} - 1}{A^{TR} \cos(qs) + B^{TR} - 1} \right]. \quad (6)$$

One can then calculate the magnetization state after the β pulse in the steady state

$$M_z^{SS,\beta}(s) = [A^\beta \cos(qs) + B^\beta] M_z^{SS}(s) + C^\beta M_0 \quad (7)$$

and after TB

$$M_z^{SS,TB}(s) = [A^{TB} \cos(qs) + B^{TB}] M_z^{SS}(s) + C^{TB} M_0. \quad (8)$$

We show graphs of Eqs. (6)–(8) in Fig. 2 for TR = 2 s.

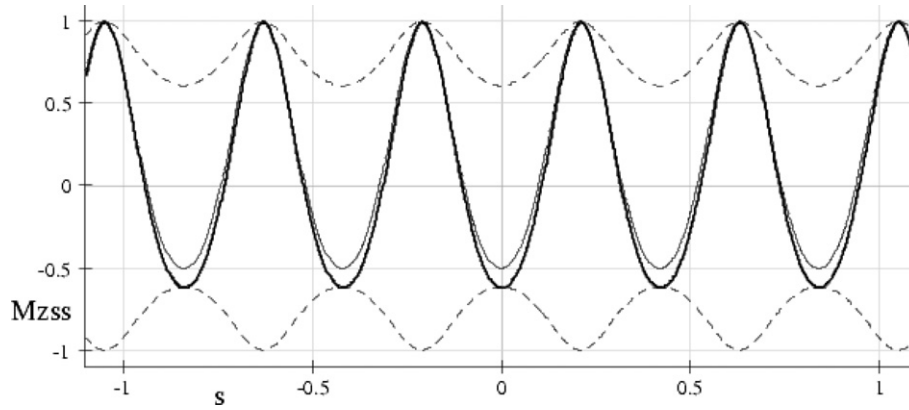


Fig. 2. Theoretical values of $M_z(s)$. $M_z^{SS}(s)$ is shown dashed (---) as an envelope, $M_z^{SS,\beta}(s)$ is shown as a heavy line, $M_z^{SS,TB}(s)$ as a normal line. $\alpha = \beta = 90^\circ$, TR = 2 s, TM = 0 ms, TB = 100 ms, and $T_1 = 1.4$ s.

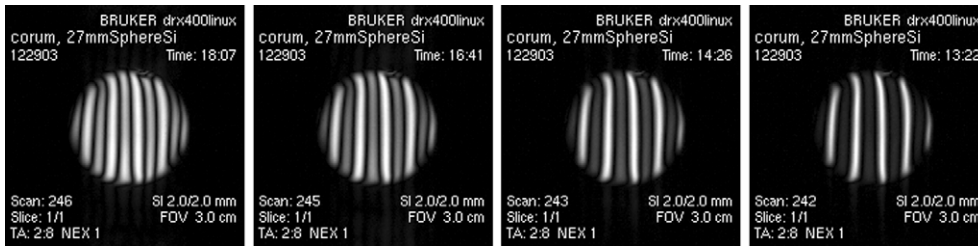


Fig. 3. $M_z^{SS}(s)$ images, Scan 246, TR = 5 s; Scan 245, TR = 2 s; Scan 243, TR = 1 s, and Scan 242, TR = 500 ms. TM = TB = 7 ms and relax = 10 s for all images.

Row 128 Data and Theoretical Curves

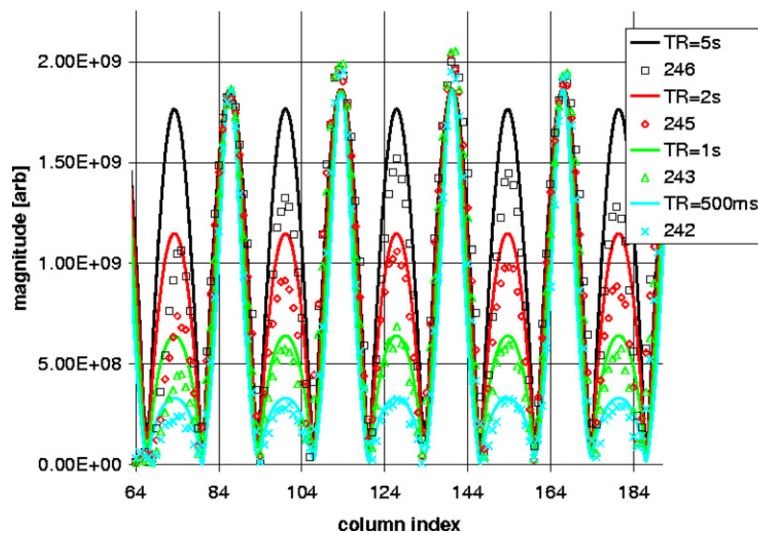


Fig. 4. Row 128 data (points) and fit (lines) $\alpha = \beta = 90^\circ$, TR = 2 s, TM = TB = 7 ms, and $T_1 = 1.4$ s, and relax = 10 s.

4. Results

We now show in Fig. 3 representative $M_z^{SS}(s)$ magnitude images obtained with the sequence described in Section 2 for four different values of $TR = 5$ s, 2 s, 1 s, and 500 ms. Fig. 4 shows several cross sections through row #128 of Fig. 3. The object is an 18 mm glass sphere filled with silicone oil. Data points are superimposed with the corresponding magnitude of the theoretical curve. The T_1 of the silicone oil (at 400 MHz) was measured by spectroscopic inversion recovery to be 1.4 s. A Bruker DRX400 Micro 2.5 system was used with a custom 27 mm diameter ^1H birdcage coil. Ten TR periods were used to establish steady state. A 10 s “relax” delay was used between phase encodes to establish full relaxation. G_q was 3 ms and 2.5 mT/mm, with G_{spoil} of 5 ms and 100 mT/mm. No attempt was made to account for B_1 inhomogeneity. A single scaling parameter was used for all theoretical curves. We achieved good agreement with the theoretical predictions. In the sequence as used $TM = TB = 7$ ms. A variety of other G_q directions and strengths show similar agreement with theory. Better agreement in the fit between experiment and theory can be obtained with $\alpha = \beta = 75^\circ$ than with the nominal 90° . A B_1 map needs to be determined to see if this corresponds more closely to the actual experimental conditions.

5. Conclusions

The expressions developed and verified above should be useful to those wishing to understand or utilize harmonics in the $M_z^{SS}(s)$ profile in DDF based sequences in the situation where the diffusion distance during TR compared with λ is negligible. This is especially true for those carrying out structural measurements which depend on a well defined correlation distance. The theory should also hold for spatially varying magnetization density $M_0 = M_0(\vec{r})$, and longitudinal relaxation $T_1 = T_1(\vec{r})$.

Acknowledgments

This work and preparation leading to it was carried out under the support of the Flinn Foundation, a State of Arizona Prop. 301 Imaging Fellowship, and NIH 5R24CA083148-05.

References

- [1] G. Deville, M. Bernier, J. Delrieux, NMR multiple echoes observed in solid ^3He , Phys. Rev. B 19 (11) (1979) 5666–5688, Available from: <<http://dx.doi.org/10.1103/PhysRevB.19.5666>>.
- [2] R. Bowtell, R.M. Bowley, P. Glover, Multiple spin echoes in liquids in a high magnetic field, J. Magn. Reson. 88 (3) (1990) 641–651.
- [3] I. Ardelean, S. Stapf, D. Demco, R. Kimmich, The nonlinear stimulated echo, J. Magn. Reson. 124 (2) (1997) 506–508, Available from: <<http://dx.doi.org/10.1006/jmre.1996.1081>>.
- [4] Q. He, W. Richter, S. Vathyam, W. Warren, Intermolecular multiple-quantum coherences and cross correlations in solution nuclear magnetic resonance, J. Chem. Phys. 98 (9) (1993) 6779–6800, Available from: <<http://dx.doi.org/10.1063/1.464770>>.
- [5] S. Ahn, N. Lisitza, W. Warren, Intermolecular zero-quantum coherences of multi-component spin systems in solution NMR, J. Magn. Reson. 133 (2) (1998) 266–272.
- [6] C.A. Corum, A.F. Gmitro, Effects of T2 relaxation and diffusion on longitudinal magnetization state and signal build for HOMOGENIZED cross peaks, in: ISMRM 12th Scientific Meeting, International Society of Magnetic Resonance in Medicine, 2004, Poster 2323, $\cos(\beta)$ should be $(\cos(\beta)+1)/2$ in abstract. URL <http://arxiv.org/abs/physics/0406051>.
- [7] R. Bowtell, P. Robyr, Structural investigations with the dipolar demagnetizing field in solution NMR, Phys. Rev. Lett. 76 (26) (1996) 4971–4974, Available from: <<http://dx.doi.org/10.1103/PhysRevLett.76.4971>>.
- [8] W. Warren, S. Ahn, M. Mescher, M. Garwood, K. Ugurbil, W. Richter, R. Rizi, J. Hopkins, J. Leigh, MR imaging contrast enhancement based on intermolecular zero quantum coherences, Science 281 (5374) (1998) 247–251, Available from: <<http://dx.doi.org/10.1126/science.281.5374.247>>.
- [9] F. Alessandri, S. Capuani, B. Maraviglia, Multiple spin echoes in heterogeneous systems: physical origins of the observed dips, J. Magn. Reson. 156 (1) (2002) 72–78, Available from: <<http://dx.doi.org/10.1006/jmre.2002.2543>>.